MQP-BC-DSA-1120

DESIGN OF A PLASMID EXPRESSION SYSTEM FOR SIMULTANEOUSLY CO-EXPRESSING HIGH LEVELS OF MULTIPLE GLOBIN SUBUNITS

A Major Qualifying Project Report

Submitted to the Faculty of the

WORCESTER POLYTECHNIC INSTITUTE

in partial fulfillment of the requirements for the

Degree of Bachelor of Science

in

Biochemistry

by

Matthew Kizner

January 9, 2008

APPROVED:

William Royer, Ph.D.
Biochemistry and Mol. Pharmacology
UMass Medical Center
Major Advisor

David S. Adams, Ph.D.
Biology and Biotechnology
WPI Project Advisor

ABSTRACT

The heterotetrameric hemoglobin (HbII) from the blood clam *Scapharca inequivalvis* assembles from two heterodimers and provides a simple system to analyze the allosteric mechanisms in which unlike subunits bind ligands cooperatively. By finding a more effective way to produce HbII in lab, as well as HbI, the homodimeric hemoglobin from the same organism, work can continue forward on the allosteric and kinetic studies of this interesting protein.

TABLE OF CONTENTS

ACKNOWLEDGEMENTS

I would like to start by thanking Dr. William Royer for allowing me to work in his lab, for his constant guidance in areas both related and not related to the project, and for his taking a chance on a student with a lot to learn. I would also like to thank lab manager Michael Omartian. His patience, boundless ability to teach and inspire, and answering of late night phone calls about mundane procedures were integral to the success of the project. I would also like to thank Dr. Song Tan (Associate Professor of Biochemistry and Molecular Biology, Penn State University) for usage of pST39, as mandated by our search for a better expression system. I would also like to thank Dr. Anthony Poteete, University of Massachusetts Medical School (Summerford, 1995) for the use of pCS26, the plasmid that inspired and was used to model all aspects of this project. Lastly, I would like to thank Dr. David Adams of Worcester Polytechnic Institute for being my WPI Project Advisor. His perspective and advice were integral in the project's success and the editing of the final report, which could have never happened without him.

BACKGROUND

Introduction

Scapharca inequivalvis is an arcid clam originally from the Indian-Pacific Ocean region. In the late 1960s, it settled in the middle of the Adriatic Sea's coastlines, and ecological competition ensued with the native mollusk, *Venus gallina.* Ultimately, the *Scapharca* won, leading to the progressive disappearance of *Venus gallina* (Ghisotti & Rinaldi, 1976). Early hypotheses for the *S. inequivalvis* dominance focused on the advantage given by hemoglobins present in *S. inequivalvis*, but not *V. gallina* in the sometimes limited amount of oxygen available on Adriatic Coasts and seas due to algal growth. The higher oxygen binding capacity of *S. inequivalvis* hemoglobin's HbI and HbII also began drawing some biochemical interest (Chiancone et al, 1981) in a story that interestingly points to subunit cooperativity.

Hemoglobin Structural History

Proteins from the hemoglobin family have been among the most studied of all biological proteins, with investigations dating back to the late 1800s. Even before any structures had been elucidated, Haurowitz provided the first indisputable evidence for hemoglobin structural changes based on ligand (oxygen) binding (Haurowitz, 1938). A suspension of deoxy hemoglobin crystals was made, and then oxygen was allowed to diffuse over them. The crystals broke, indicating the structures were not isomorphous, thus some sort of movement within the molecule as a result of the oxygen binding had caused the crystals to shatter.

How and why hemoglobin structure changed was soon answered using x-ray diffraction by a team led by Max Perutz. The overall molecular design (Figure-1), including the arrangement of the polypeptide chains and position of the heme groups was first published in 1962 (Cullis et al, 1962).

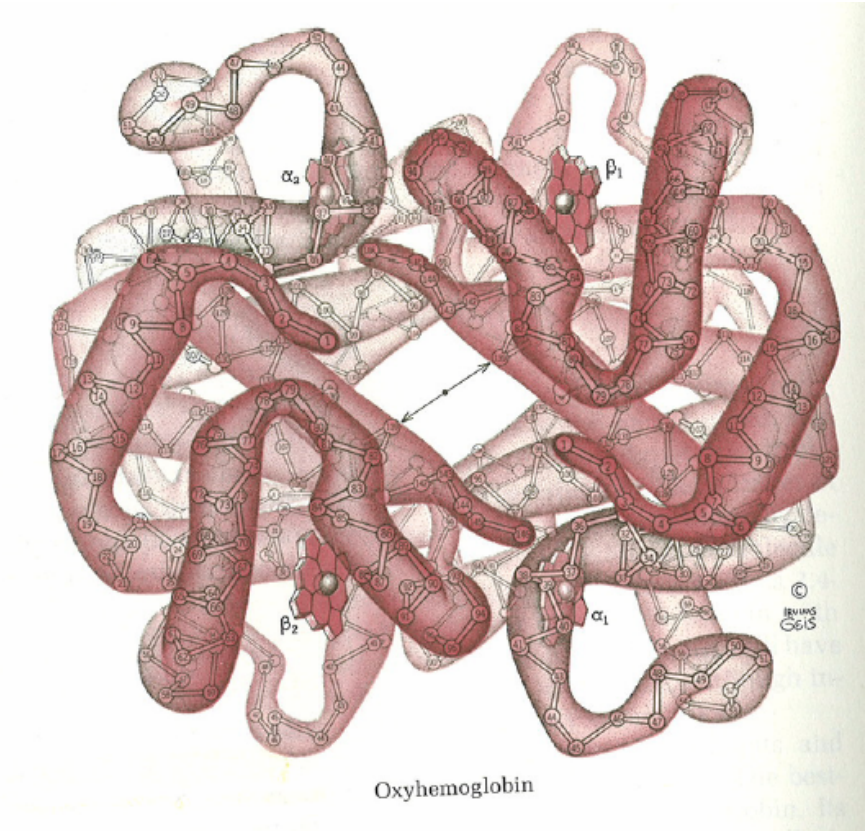

Figure-1: The Three Dimensional Structure of Oxyhemoglobin Revealed by X-Ray Diffraction Analysis. The quaternary structure is shown with the subunits in pairs (α1β1 and α2β2). The residue numbers are indicated in each chain. The heme groups are relatively far apart. Figure from Dickerson and Geis, 1982.

This approach demonstrated that each chain was globular, and possessed a highly helical structure similar to that of myoglobin, a pigment found in the muscles of animals. The structures inspired a series of x-ray and optical studies on both myoglobin and hemoglobin. Four hemoglobin chains were observed to form a tetrahedron, with close contacts between the pairs, and heme groups located at the corners of the tetrahedron on

the surface of the molecule, enveloped by polypeptide chains (Kendrew et al, 1961; Beychok et al, 1961).

Antonini went on to demonstrate it was possible to separate the heme from the protein (the α and β chains), and to isolate the various components. When this was completed, it was then possible to reform the original protein very quickly by mixing the previously isolated components in stoichiometric amounts. This approach proved the reassembling of a complete hemoglobin molecule from its components was spontaneous, fast, and a highly specific process (Antonini, 1967).

Hemoglobin Component Cooperativity Upon Ligand Binding

Interestingly, the single protein chains (globin) and the heme itself proved to have very different properties in isolation in comparison to the full molecular assemblage. This led to a major statement on the possibilities of component cooperativity, specifically that the alpha-beta dimer might be the basis for cooperativity, from Antonini. "Thus hemoglobin may be visualized as a system in which the polypeptide chains, the heme, and the iron ligands undergo reversible modifications in kind as a result of specific binding and interactions among all the components (Antonini, 1967)."

Cooperativity of binding was developed further when Perutz proved just why the deoxygenated crystals in Haurowitz's lab broke under exposure to oxygen. X-ray analysis of oxy and deoxy hemoglobin crystals showed that the positions of subunits are different in the two forms of the protein. Upon deoxygenation, the β chains move away from each other and out from the center of the tetramer. The distance between iron atoms also increases upon deoxygenation as a result of the increased distance between the β

chains. These results proved a direct, conformational change as a result of ligand binding (Perutz et al, 1964).

Conformational change as a result of ligand binding was further studied by oxygen disassociation experiments (Figure-2). The oxygen-disassociation curve for hemoglobin is sigmoidal in shape, and the affinity for oxygen increases as the saturation increases. These interesting curves ultimately lead to structural analysis of the alternate states.

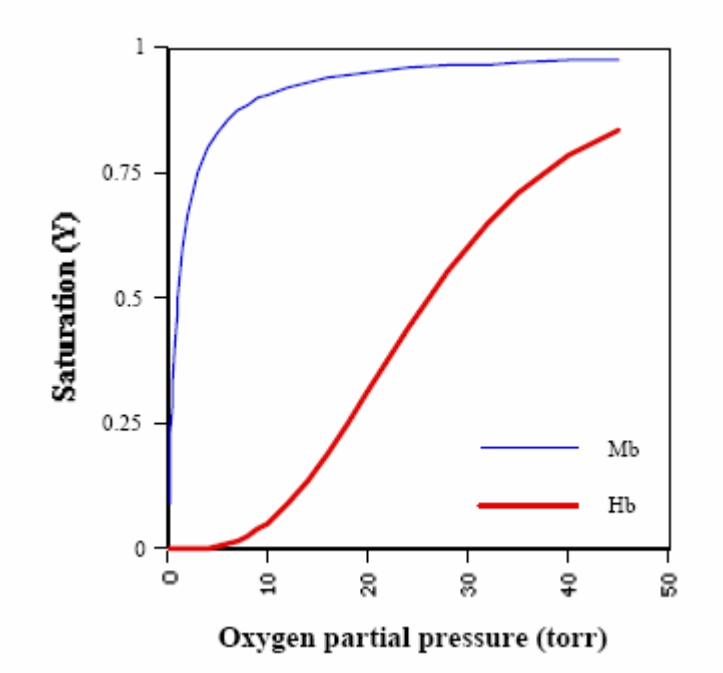

Figure-2: Oxygen Dissociation Graph for Myoglobin and Hemoglobin. The Myoglobin in blue represents the classic hyperbolic binding curve, while Hemoglobin, in red, illustrates the sigmoidal curve expected from compounds such as HbI and HbII where cooperative binding is observed. Figure from Dr. Royer, personal communication.

Antonini sums it up by stating, "The sigmoid character of the equilibrium curve implies that the affinity of the oxygen-binding sites changes as a result of the presence of the ligand on the other sites" (Antonini, 1967). While no model was available at the time to prove his theory right, he had proven that component cooperativity in ligand binding existed in hemoglobin, and even stated the conditions that could affect binding based on

the medium, such as pH, the Bohr Effect (Bohr et al, 1904), salt concentration, or the presence of CO_2.

Antonini also did some kinetic work on the hemoglobins, with a goal of finding a way to elucidate the mechanism by which cooperative binding occurs. Unlike myoglobin, hemoglobin demonstrated different kinetic tendencies as a result of photolysis compared to those observed in the rapid mixing experiments (Gibson, 1959). It was observed that the flash photolysis was characterized by a rapid phase because of material reacting with ligand much faster than that of hemoglobin (Antonini, 1967). Antonini could not explain the phenomenon of the two different tests resulting in different kinetics, or even why his studies showed hemoglobin reacting the way it did, nor could any of his contemporaries. He did observe that there is no change in the kinetics of hemoglobin reactions when it is disassociated into dimers, indicating that the kinetic features of hemoglobin may only be attributed to the AB dimer (Antonini, 1967). More complex answers and mechanisms for the concept of intradimer cooperativity would not come for nearly 4 decades.

S. inequivalvis **Hemoglobin**

The next key step in analyzing hemoglobin function resulted from the analysis of hemoglobins showing strong cooperative binding tendencies, such as the hemoglobins of *Scapharca inequivalvis*. These studies came in 1981 from a team consisting of Chiancone, the aforementioned Antonini, and others who showed that a dimer could bind cooperatively through interpretation of equilibrium experimentation, using data from circular dichroism, and most tellingly, observations of the association-dissociation phenomenon via sedimentation velocity experiments (Chiancone et al, 1981).

Sedimentation velocity is a measure of speed resulting from the force felt by a given molecule as a result of differential centrifugation. Four key factors affect sedimentation velocity (measured in Svedberg units): size, shape, mass, and density, and each affects the sedimentation velocity in a fairly predictable manner. The sedimentation velocity of oxy HbI (discussed later) corresponds to.2.7S (Svedberg units), and is unchanged by the removal of oxygen over the pH range 5 to 9 (Chiancone et al, 1981). Similarly, oxy HbII has an unchanged sedimentation coefficient of 4.3S over the previously noted pH range. The outlier comes from the deoxygenation of the samples at physiological pH. In a solution of high protein concentrations at physiological pH, the deoxygenated samples polymerize to a component of 8 to 10 S. This polymerization reverses upon reoxygenation of the samples. The only way the sedimentation velocity of the globins could have changed under these conditions would be if the actual structure of the proteins themselves changed. Through interpretation of sedimentation velocities as well as functional binding experiments, it can be said that removal of the oxygen ligand coupled with the globin at a high concentration resulted in the protein assembling into a higher molecular complex that, based on linkage theory in a cooperative system, would be expected to have lower oxygen affinity. The reversal of the polymerization upon reoxygenation only further supports this conclusion, showing that the protein has shifted to a high affinity state as the majority of proteins in solution have bound ligand, in this case, oxygen.

On the whole, the oxygen affinity of the two hemoglobins is similar at physiological and alkaline pH levels, where the Bohr effect is not a factor. When dealing with slightly acidic pH values, the tetramer has a higher oxygen affinity than the dimer

due to a small acid Bohr Effect (Chiancone et al, 1981). This led to a series of kinetic studies to be published at a later date by Antonini, in which he strived to prove the cooperativity of dimers through non equilibrium kinetics experiments.

Antonini and colleagues continued the exploration of cooperativity of binding in *S. inequivalvis* by a non equilibrium kinetics experiment using flash and dye-laser photolysis. Using the allosteric model to be discussed in the structural section to follow, first proposed by Monod (Monod et al, 1965), they observed the kinetics of ligand binding to HbI based on whether it was in the T state, a low affinity, "tense" state, or if it was in the R state, a high affinity, "relaxed" state.

The first foray into the kinetics of oxygen binding to *S. inequivalvis* HbI was studied by photodissociation. The oxygen combination rate constant was measured by flashing an HbICO solution in the presence of oxygen at 120 μM. The process was a second order reaction, and the experimentally determined rate constant for the overall oxygen combination varied between 12 and 15 μM per second. This data showed that combination with oxygen of both partially and totally photodissociated $HbIO_2$ yielded values that were almost identical. Photodissociation on 100% saturated hemoglobin using a dye-laser system showed that recombination was closely proportional to oxygen combination, and there was no difference in rate after full and partial photolysis at high oxygen concentrations (Antonini et al, 1984).

Photodissociation was also carried out with carbon monoxide, using different extents of photodissociation, ranging from 100-5%, with CO concentrations ranging from 7-1000 μM, and HbI concentrations of about 1-75 μM. An accelerating time course of binding was observed (Figure-3) following 100% photodissociation, with a rate constant

of about 7-10 micromolar per second of CO binding. Interestingly, when photo-dissociation was less than 70%, reaching its peak at 10% photodissociation, a rate constant of 20 μM per second of CO binding was observed. "This increase in the CO combination velocity constant as the reaction proceeds may be considered the kinetic counterpart of cooperativity in CO binding to HbI" (Antonini et al, 1984).

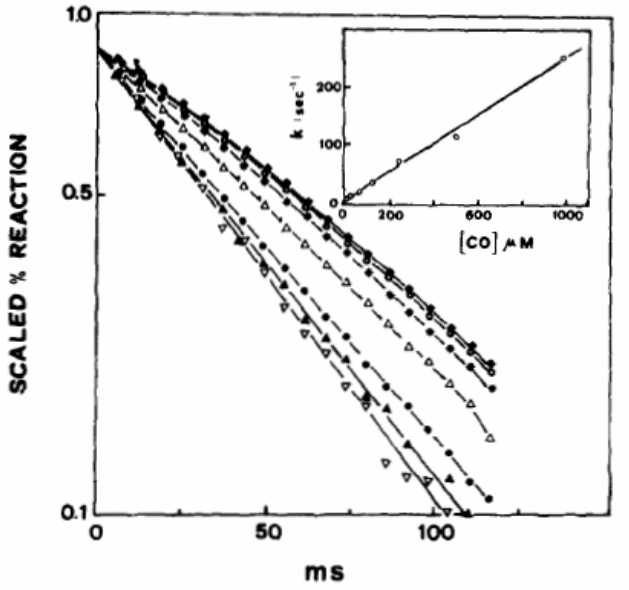

Kinetics of CO combination with *S. inaequivalvis* HbI following flash photolysis of HbICO. Different *symbols* refer to the time course of the combination reaction after different degrees of photodissociation: ■, 100%; ○, 97%, *, 83.3%; △, 59.7%; ●27%; ▲, 13.7%, ▽, 6.6%. Protein concentration, 4 μM; CO concentration, 92 μM. 0.1 M phosphate buffer, pH 7.0, 20 °C. Observation wavelength, 435 nm. The results are presented as scaled semilogarithmic plots covering 90% of the reaction. The *inset* shows the results of partial photolysis (2.5%) at different CO concentrations.

Figure-3: Analysis of *S. inequivalvis* Hemoglobin Kinetics of Binding Carbon Monoxide Following Flash Photolysis of HbICO. Different symbols refer to time course of combination reactions after different degrees of photodissociation. Square- 100%, White circle 97%, Asterisk 83.3%, White triangle 59.7%, Black Circle 27%, Black Triangle 13.7%, Upside down white triangle 6.6%. Figure is from Antonini et al, 1984.

The last set of experiments involved laser photolysis at or near the isobestic point during ligand rebinding (Figure-4). On full flash, effectively removing all CO on a short time scale, the deoxy-HbI attains a T state conformation. Binding to the T state, thus, is observed as the ascending limb of the trace, shown below. The max binding potential of the T state is reached after ~10 ms, and then declines as future binding of molecules of ligand is associated with a change from the T to R state, that is to say, at full photolysis,

binding to the T state takes place initially, followed by additional binding and conversion to the R-liganded form (Antonini et al, 1984).

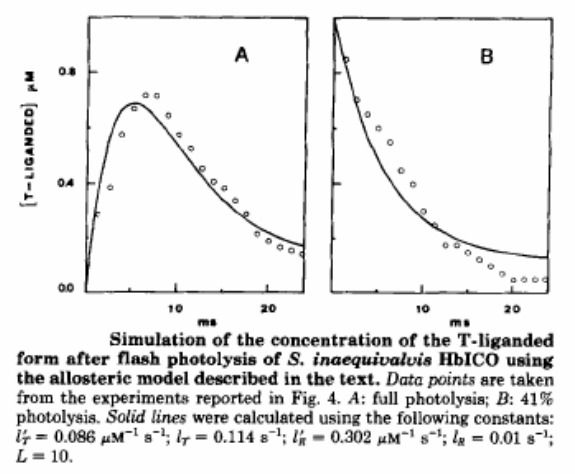

Simulation of the concentration of the T-liganded form after flash photolysis of *S. inaequivalvis* HbICO using the allosteric model described in the text. *Data points* are taken from the experiments reported in Fig. 4. *A*: full photolysis; *B*: 41% photolysis. *Solid lines* were calculated using the following constants: $l'_T = 0.086\ \mu M^{-1}\ s^{-1}$; $l_T = 0.114\ s^{-1}$; $l'_R = 0.302\ \mu M^{-1}\ s^{-1}$; $l_R = 0.01\ s^{-1}$; $L = 10$.

Figure-4: Analysis of *S. inequivalvis* Hemoglobin by Simulation of the Concentration of the T-Liganded From After Flash Photolysis Using the Allosteric Model. Figure A, full photolysis, illustrates the ascending limb of binding to the T state after full flash, with the peak serving as an illustration for confirmation change. Figure B, a partial flash of 41%, illustrating the lack of conformational change. Figure is from Antonini et al, 1984.

When partial flash occurs, the biggest difference is in the ascending limb. In each of the three observed fractions of photolysis, there is an immediate increase in absorbance (Figure-5). The HbI with one ligand remaining rapidly rearranges from the R to the T state, accounting for the immediately observed absorbance. In other words, with partial photolysis, the liganded T state is immediately populated within the flash by the flash, and then decays to the liganded R state upon addition of more ligand (Antonini et al, 1984).

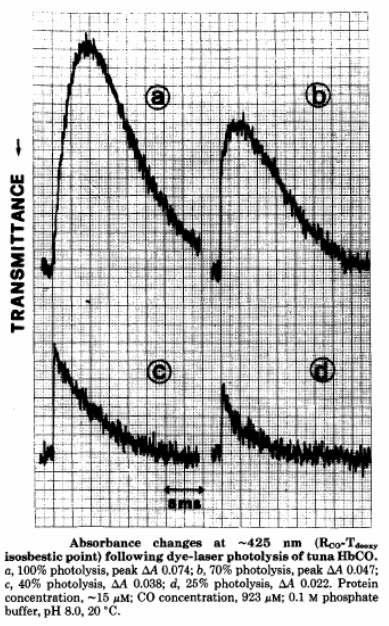

Absorbance changes at ~425 nm (R_{CO}-T_{deoxy} isosbestic point) following dye-laser photolysis of tuna HbCO. *a*, 100% photolysis, peak ΔA 0.074; *b*, 70% photolysis, peak ΔA 0.047; *c*, 40% photolysis, ΔA 0.038; *d*, 25% photolysis, ΔA 0.022. Protein concentration, ~15 μM; CO concentration, 923 μM; 0.1 M phosphate buffer, pH 8.0, 20 °C.

Figure-5: Analysis of S. inequivalvis Hemoglobin by Absorbance Changes at 425 nm Following Dye-Laser Photolysis. A is 100% photolysis. B is 70% photolysis. C is 40% photolysis. D is 25 % photolysis. Decrease in ascending limb directly correlates with decrease in % photolysis, suggesting that ligand rebinds faster when no conformational change is made or required as a result of photolysis. Figure taken from Antonini et al, 1984.

The results of these experiments, in Antonini's own words, "indicate that a ligand linked quaternary change postulated on the basis of the cooperative oxygen binding can actually be demonstrated." With cooperativity of ligand binding for *Scapharca inequivalvis* hemoglobin proven via equilibrium and non equilibrium experimentation, much of the work of the 1990's would focus on elucidating structural mysteries, such as the actual mechanism for cooperativity.

Recent Resurrection of the Hemoglobin Intradimer Cooperativity Hypothesis

The most recent and intriguing piece of evidence supporting hemoglobin intradimer cooperativity came in 2002 from Gary Ackers and colleagues. Thermodynamic analysis of hemoglobin dissociation as a function of ligand state has provided some evidence supporting intradimer cooperativity within the context of the hemoglobin tetramer, resurrecting the 30 year old hypothesis from Eraldo Antonini. In the case of human hemoglobin, initial binding of oxygen to the heme Fe drives

intrinsically unfavorable conformational change within the globin. This energy penalty results in a lower binding constant for initial ligation. Each progressive binding of ligand has a reduced energy penalty, yielding Hb's distinctive sigmoidal curve (Ackers et al, 2002).

The energetic penalty as a result of ligand binding the tetramer was given a value, as the free energy difference between each tetrameric species having bound oxygen in a specific site configuration and the corresponding set of dimeric reference species. This value was represented as ΔGc, the cooperative free energy penalty. Therefore, Hb cooperativity is the stepwise decrease in ΔGc penalty with successive oxygen bound (Ackers et al, 2002).

Ackers ran various thermodynamic and kinetics experiments on the Hb tetramer in various states of oxygen ligation. Experiments done with the Hb tetramer with one dimer unligated, and the other dimer fully ligated, gave an interesting ΔGc penalty compared to the other observed species. This phenomenon forms the basis for what Ackers believes to be "a microstate model of cooperativity in which the Hb tetramer functions as a dimer of cooperative αβ dimers" (Ackers et al, 2002).

In order to observe this phenomenon, Ackers decided to make a modification of one dimer within the tetramer, residue Arg 141, typically used to examine cross-dimer functional coupling, was enzymatically removed, eliminating two key cross-dimer salt bridges. This is important because it had been universally observed that removal of any dimer-dimer contact, be it hydrogen bonds or a salt bridge, results in an increase in oxygen affinity and a decrease in cooperativity. This led to the widely held assumption that cooperativity resulted from the global quaternary T<->R switching. In this common

view, oxygen driven subunit conformational changes are transmitted from the heme solely to the dimer-dimer interface, with no intradimer cooperativity (Ackers et al, 2002).

Results of the desArg A141 mutation were intriguing. The loss of just one A141Arg residue destabilizes the deoxy tetramer. However, only the modified dimer exhibits the increased ligand binding affinity described above, while the wild-type dimer within the modified tetramer exhibits wild-type ligand binding affinity. Similar results were found by making a B unit mutation at B99 Asp -> His, breaking two cross-dimer hydrogen bonds in the A1B2 interface. These are a result of the intradimeric response to the modification of interface contacts, rather than a cross-dimer quaternary response, flying in the face of the typically held notion of quaternary responses being the method of cooperativity (Ackers et al, 2002).

Hybrid Hbs containing one ArgA141 or B99His modifications show that removal of interdimer contacts weakens the T interface, but is not communicated from heme to heme across the interface (Ackers et al, 2002). Ackers asserts that the perturbation due to modification appears to be "long range" within the dimer itself, in that "an A-subunit modification affects the B-subunit heme within the same dimer, and a B-subunit modification affects the A-subunit heme within the same dimer" (Ackers et al, 2002). In Ackers's model, ligation to a single dimer within the tetramer yields a ΔG_c penalty without T -> R quaternary switching, which is not possible under the old T state/R state assumptions. Upon further ligation, when both dimers contain at least one ligand, the combined ΔG_c penalty exceeds the free energy of the T interface, which then rearranges to the less stable, higher affinity R state in a concerted quaternary switch (Ackers et al, 2002). Unlike in the T state/ R state model, ligands bind cooperatively to a single dimer

within the tetramer, followed by a single concerted quaternary switch, and subsequent cooperative ligation by the other dimer (Ackers et al, 2002).

If true, Ackers's assertions would change the entire way cooperativity is viewed within vertebrate hemoglobins. In contrast, work as far back as 1985 has suggested that each half of *Scapharca* HbII might be cooperative. Traditional notions on cooperativity viewed Hb function as a tetramer of four similar subunits that bind cooperatively as a tetramer, rather than as a dimer of cooperative AB dimers, as Antonini had first proposed 35 years prior.

With such a diverse history of research already done, and so much left to be learned, it's easy to see why HbI and HbII are used as model systems to study protein cooperativity, kinetics of ligation, and structural mechanics.

S. inequivalvis HbI and HbII and Subunit Cooperativity

Many kinds of hemoglobins exist in the animal kingdom, but for the purposes of this MQP project three specific types were analyzed. The majority of the project analyzed *Scapharca inequivalvis,* a clam with two different types of hemoglobins in its blood. Hemoglobin-I (HbI) exists as a homodimer (consisting of two identical interacting subunits), represented by Figure-6. Hemoglobin-II (HbII) exists as a heterotetramer, (termed a heterotetramer because the tetramer is made of unlike subunits). The heterotetramer shown in Figure-7 consists of two cooperatively interacting dimer subunits, with each dimer assembled from two non-identical subunits, called A and B. HbII is made of two cooperative AB heterodimers, whereas HbI consists of just one singular AA homodimer. The third hemoglobin analyzed was human hemoglobin, HbA,

used extensively for comparisons. Early work on human HbA led to a major misconception, when researchers interpreted early experimental results as being more indicative of the norm rather than the exception, resulting in the belief that interactions between unlike human globin subunits were essential for hemoglobin cooperativity. Subsequent observations of the simpler assembly of *Scapharca* HbI homodimers changed all that, irrefutably demonstrating that different subunits are not required for cooperative ligand binding.

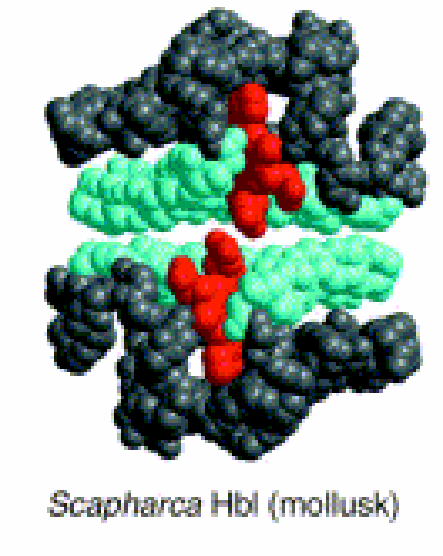

Figure-6: Diagram of *S. inequivalvis* Hemoglobin-I Homodimer. Two homosubunits are shown in gray. E/F helices are shown in cyan, and heme is in red. This figure provides an excellent visualization of what HbI looks like, taking effort to accentuate the placement of the heme in the heme pocket, and the role the E/F helices play in keeping them there. Figure from: Royer, Personal Communication.

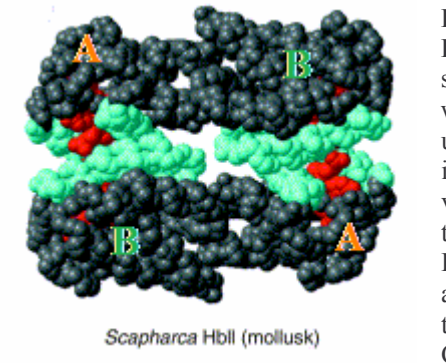

Figure-7: Diagram of *S. inequivalvis* Hemoglobin-II Heterotetramer. The four subunits are shown in gray. The A subunits have been labeled with Orange A's, and the B subunits with Green B's to illustrate how the heterodimers assemble and ultimately bind to form the heterotetramer. E/F helices are shown in cyan, and heme is in red. This figure provides an excellent visualization of what HbII looks like, taking effort to accentuate the placement of the heme in the heme pocket, and the role the E/F helices play in keeping them there. The figure also provides an excellent visualization of how the subunits bind to each other to form the heterodimers. Figure is from Royer, Personal Communication.

Figure-8 shows a different view of the *S. inequivalvis* HbI subunit, with a focus on the arrangement of the E and F helices, alpha-helical domains that form the heme pocket that binds heme. This different view provides an up close look at the cyan helices from Figure-6. The diagram illustrates how the position of the helices helps form the "heme pocket" required for the homodimer, and specifically the EF dimer assemblage shown in Figure-8, to bind the heme, shown in red.

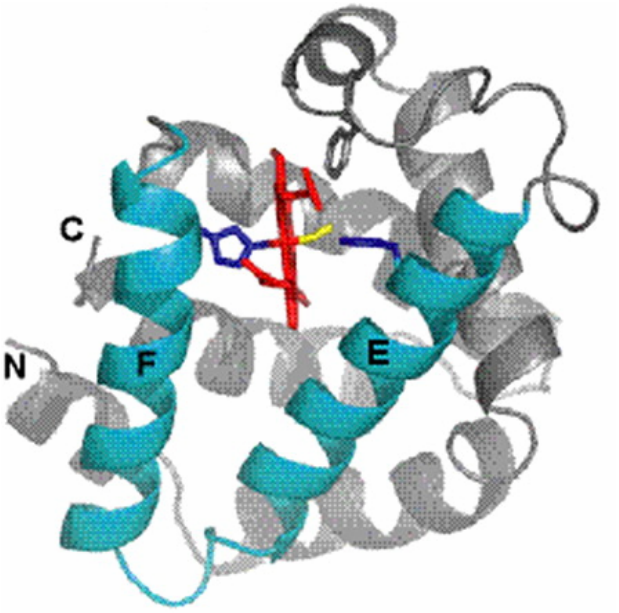

Figure-8: Diagram of S. inequivalvis HbI Individual Subunit. This figure illustrates the positioning of the E and F helices to form the heme pocket. Figure is from Royer, Personal Communication

Figure-9 shows a different view of the *S. inequivalvis* HbI homodimer, focusing on cooperation between the E and F helices. Cooperative binding between the two identical subunits is shown at two duplicate sites. The *S. inequivalvis* E and F helices were found to actually bring the heme groups into close range, allowing for more direct interaction than in most mammalian hemoglobins. This construct was termed the EF dimer, and has been found in hemoglobins as small as two subunits to as large as 144 subunits.

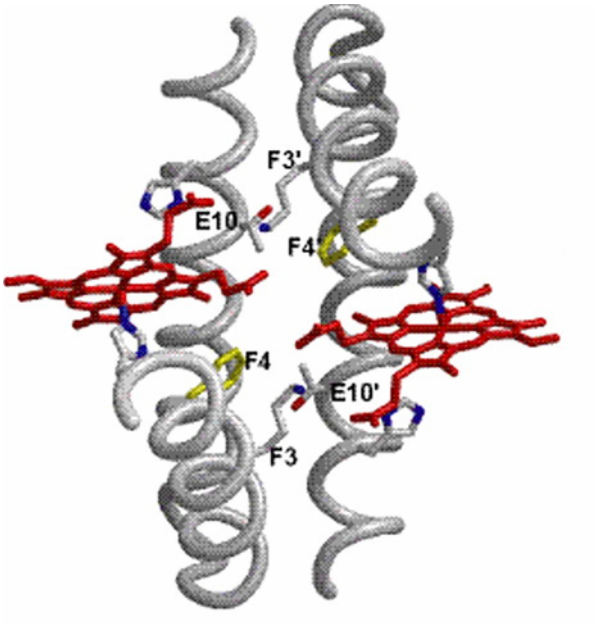

Figure-9: Diagram of S. inequivalvis Hemoglobin-I E and F Helices With Bound Heme. This is a direct visualization of the E-F helices, paying specific attention to the residues important in binding of ligand and formation of the heme pocket. Royer, Personal Communication

HbII is actually present in higher quantities than HbI, and shows cooperative oxygen binding with hill coefficients of 1.9-2.1, a higher rate than the 1.5 observed in HbI. Unlike HbI, HbII forms itself into heterodimeric subunits, made of one Asubunit and one Bsubunit. These heterodimers then bind with a second heterodimers to form the heterotetramer that makes HbII such an interesting specimen to study. In essence, each side of the tetramer is made of a unique IIA-IIB EF dimer, displaying a similar assembly with respect to the previously discussed HbI homodimer. This striking similarity to the HbI homodimer led to the discovery that all residues used in the cooperative binding mechanism of HbI are conserved in HbII, suggesting each HbII heterodimer may function similarly to their evolutionary HbI homodimer cousin (Royer, Personal Communication).

One of the key points addressed was why the HbII favored heteromeric pairing over homomeric pairing, that is to say, why did HbII form AB dimers instead of AA and BB dimers as a precursor for tetramer formation? In order for this to happen, something must actively weaken the homomeric affinity of the individual subunits for each other.

Hemoglobin Ligand Binding and Allostery

Allosteric mechanisms have a variety of means to regulate the processes of a biological system. One of the main ways this is done is through ligand transport and binding. High resolution analysis revealed significant changes to the tertiary structure of various hemoglobins based on whether the ligand was bound or unbound (Figure-10).

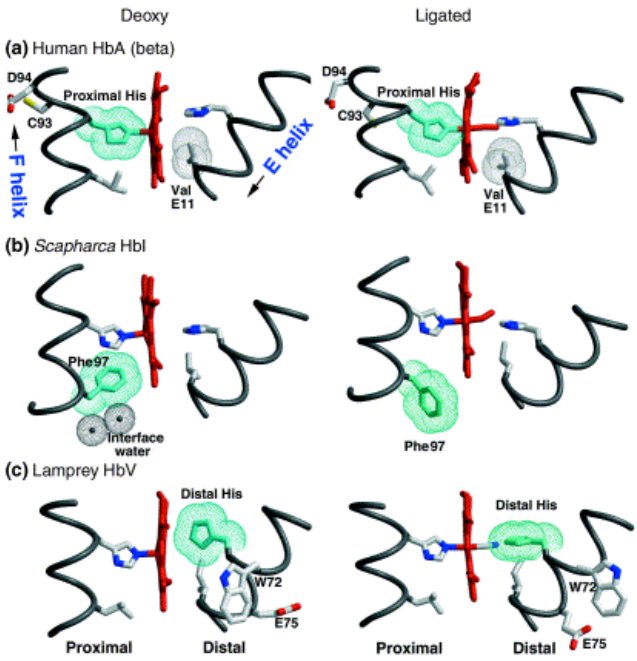

Figure-10: Diagram of Various Hemoglobins Detailing Conformational Changes as a Result of Ligand Binding. The figure shows the effect of oxygen binding to the various deoxy forms of hemoglobin. Royer, Personal Communication.

One major change upon ligand binding to Scapharca HbI is the movement of Phe97 from the heme pocket into the interface post ligand binding. This helped elucidate that the low affinity of the deoxy state (unliganded) was a result of the packing of the Phenylalanine side chain into the heme pocket. This Phe restricts heme iron movement, but also serves to elongate a key hydrogen bond involving the proximal Histidine, further illustrating how control of iron reactivity plays a pertinent part in controlling ligand affinity (Knapp et al, 2005).

Yet this still leaves the question of how the allosteric signal is proliferated among the subunits. It was observed that the non ligand bound structure of HbI has an ordered

water cluster in the subunit interface that helps stabilize the low affinity form of each subunit. However, it is notable that the ligand induced movement of the Phe97 disrupts the water cluster, yielding a smaller and less ordered water interface. It was hypothesized that disrupting this water pocket could be the signal that one subunit used to notify its "partner" of its ligand state. This hypothesis was tested by disrupting the water cluster via mutagenesis and osmotic induced stress, and both methods led to an overall increase in oxygen affinity. This proved a direct relationship between the interface water structure and oxygen affinity with respect to cooperative function between subunits (Royer et al, 1996).

In order to test some of the assumptions made above, and to answer some questions involving preference of heteromeric binding over homomeric binding, a Size Exclusion Chromatography column was run on HbII subunits (Figure-11). Three columns were run, one of isolated HbIIA, one of HbIIB, and one of IIA and IIB, that was used following an incubation of 4 hours in appropriate buffer. The results, provided below, show that while the IIA and IIB will form dimers in isolation, they will not form homotetramers (Royer, Personal Communication).

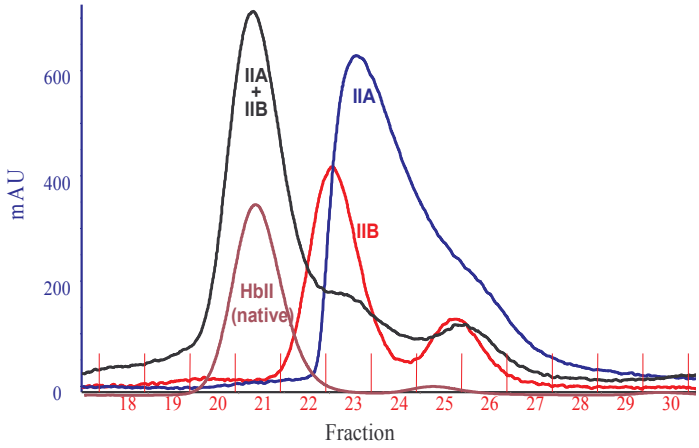

Figure-11: Size Exclusion Chromatography. Elution volume is related to the size of the assembly, with earlier elution (left side) indicative of higher assemblages. In this experiment, hemoglobins IIA or IIB by themselves show no evidence of assembling into tetramers, which require the presence of both subunits. Royer, Personal Communication.

This confirms the earlier assertion that both subunits are required to form the tetramer.

Next, isothermal titration calorimetry (ITC) was used to ascertain a deeper comprehension of the thermodynamic preference for heterodimers formation among HbII. The ITC will measure the heat released or absorbed by the formation of the various HbII subunit complexes. Purified IIA and IIB subunits were mixed via titration, and the results showed that the formation of a heterotetramer was the most enthalpically and entropically favorable. Interestingly, it is unknown if the binding of IIA and IIB subunits is energetically favorable because of their preferential binding into similar EF dimers, or because of their ability to assemble into a stable heterotetramer (Royer, Personal Communication).

In order to test the cooperativity of ligand binding, equilibrium oxygen binding measurements were taken of the isolated subunits using flash photolysis. The binding of a ligand to a macromolecule is often enhanced if there are already other ligands present on the same macromolecule, a phenomenon known as cooperative binding. The Hill coefficient, named for Archibald Vivian Hill, provides a way to quantify this effect. Both IIA and IIB were shown to have slight oxygen cooperative binding, each having Hill Coefficients, of approximately 1.2 in equilibrium binding measurements. IIA and IIB had very different oxygen affinities than WT HbII, with HbII showing a hill coefficient of 2. Upon integration of the two subunits together, there is no functional difference detected between the two subunits. They actually form a highly cooperative construct in which the two subunits have essentially lost their distinctiveness (Royer, Personal Communication).

Polycistronic Plasmid Based Expression Systems

No hemoglobin research is possible without a viable means to express the various subunits of the protein. Individual expressions of the isolated subunits previously provided rather low yields, possibly due to instability in the absence of forming a stable tetramer. A means to provide a better yield, using co-expression of the subunits was sought. The presence of both subunits is necessary for complete assembly of the tetramer to take place in *E. coli*, a phenomenon not possible without co-expression.

The concept of the polycistronic vector used to model our expression systems was initially made by Dr. Song Tan. He designed two vectors: a transfer vector pET3aTr (Figure-12) which was used as a model in this MQP for designing a similar cloning vector pMNOtr, for initially cloning various hemoglobin subunits.

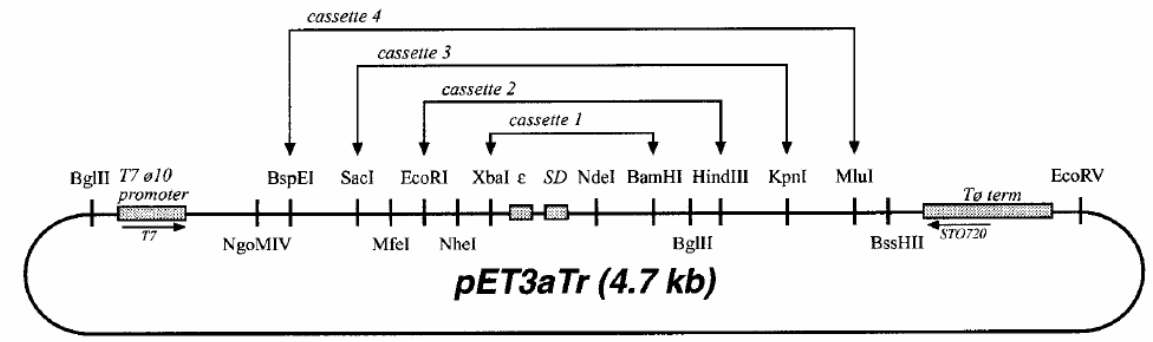

Figure-12: Diagram of Cloning Vector pER3a Tr. This plasmid was originally constructed by Song Tan (Tan, 2000). This model was used as a basis in this MQP project for creating pMNOtr, to be discussed later.

Tan's studies focused on the same goal as this MQP: Finding a better way to express multi-subunit proteins. pET3aTr served as housing for the individual genes to be expressed. Tan would insert the genes by restriction enzyme digestion into the cassettes

downstream of the ribosome binding site (RBS) (Figure-12), and remove the cassettes individually, picking up not only the desired gene to be expressed, but also obtaining a ribosome binding site essential to facilitating expression in Tan's polycistronic expression vector, pST39 (Figure-13) (Tan, 2000). pST39 contains 8 restriction enzyme sites, matching up to the cassettes in pET3aTr, allowing for easy insertion into the vector, and ultimately, co-expression of multi subunit proteins.

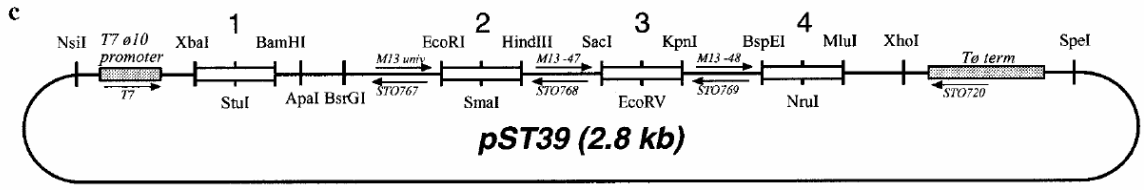

Figure-13: Diagram of Polycistronic Expression Vector pST39. This plasmid was originally constructed by Song Tan (Tan, 2000). pST39 serves as a home for the various cassettes as noted in Figure-12, and is the plasmid that was ultimately used for co-expression of multi subunit proteins.

The polycistronic vector stands in stark contrast to traditional methods of expression, which make use of a monocistronic expression mechanism (Figure-14).

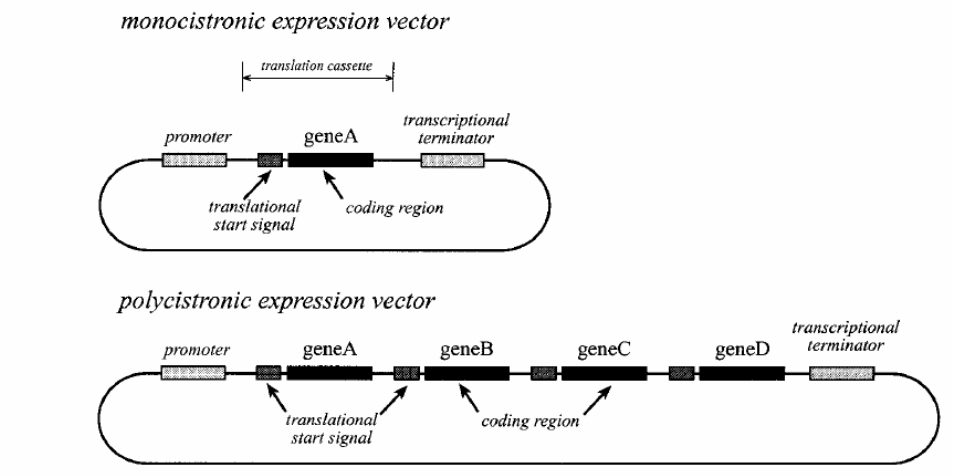

Figure 14: Example of Monocistronic Versus Polycistronic Plasmid Expression Systems. This image clearly demonstrates the difference between monocistronic and polycistronic expression vectors, visually demonstrating the one gene expressed by monocistronic systems, and the potential 4 genes that can be simultaneously co-expressed using a polycistronic expression vector with its multiple translational start domains (Tan, 2000).

The theory was that if the genes could be inserted properly into pET3aTr by means of restriction enzyme sites, they could then be cut out and placed into the pST39 at its restriction sites, each with their own ribosome binding site obtained from the transfer vector. This allows for the transcription of one, long mRNA strand as opposed to 4 different ones, which should in theory lead to a major increase in yield, efficiency, and allow for the best possible expression of multi subunit proteins, including HbII, in a lab setting, and would not require multiple antibiotics to select for each plasmid, increasing further the chances of a successful synthesis. Tan even tested the theory (Figure-15), by carrying out a co-expression with his pST39 polycistronic expression system.

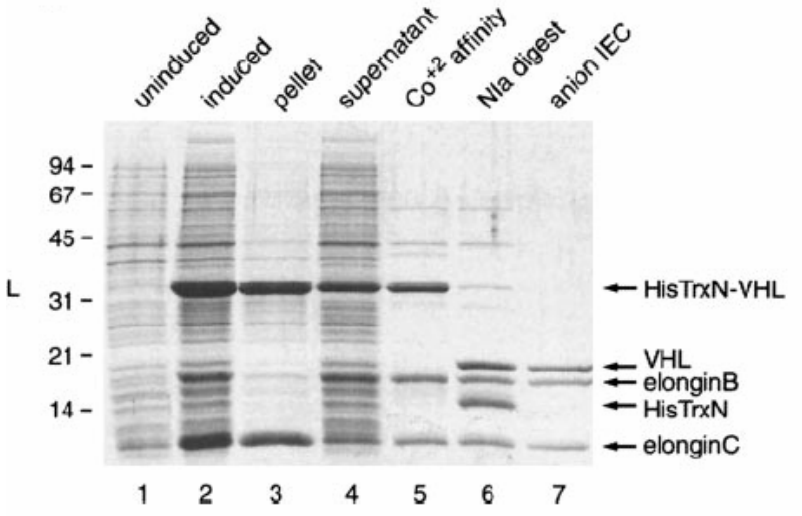

Figure 15- Coexpression of HisTrxN–VHL–elonginB and HisTrxN–VHL–elonginB–elonginC Complexes Using the pST39 Polycistronic Expression Vector. Visual confirmation of successful co-expression of different proteins using pST39 is denoted by arrows for the banding of different proteins. (Tan, 2000)

PROJECT PURPOSE

The notion of cooperativity within an αβ dimer of human hemoglobin was originally proposed by Eraldo Antonini 40 years ago (Antonini, 1967). This concept, although largely abandoned, has recently experienced a bit of a comeback due to thermodynamic experiments by Gary Ackers (Ackers et al, 2002). In light of these new subunit cooperation studies, the cooperative dimers and tetramers found in the clam *S. inequivalvis* hemoglobin are particularly interesting given the arrangement of the subunits that strongly suggests an intradimer communication within a tetramer. The purpose of this MQP is to create an effective expression system for multi-subunit hemoglobin proteins. The presence of both subunits is necessary for complete assembly of the tetramer to take place in *E. coli*, a phenomenon not possible without co-expression.

The Royer lab previously chose an expression system based on the research done by Dr. Song Tan (Tan, 2000) due to its cassette approach for creating multiple protein encoding domains, each with their own translational start site, all encoded by a single mRNA (a polycistronic approach). Unfortunately, early Royer data showed the Tan expression system ineffective for producing globins, single expressions of HbIIA and HbIIB in Tan's transfer vector, pET3aTr, provided little or no protein. In contrast, when HbIIA and HbIIB were expressed in an expression vector previously used in the Royer Lab, pCS26, a significant increase in expression levels was observed. While the reason for this observation is unclear, it is the goal of this MQP project to transform the successful monocistronic expression vector pCS26 into a polycistronic vector. By using a polycistronic plasmid vector, the co-expression required to produce efficient and stable

amounts of various unlike hemoglobin subunits will be easier to replicate in lab. Having a more efficient expression system for the various hemoglobins will allow for more research on these fascinating proteins to take place, and less downtime between the respective experiments done on them.

METHODS

Polymerase Chain Reaction Amplification

PCR reactions were performed using 1 µL of Pfu Turbo Polymerase (Stratagene), 1.25 µL of ~100 ng/uL Sense and Antisense Primers (IDT), 1 µL dNTP cocktail, 5 µL 10x Pfu buffer, 35.5 uL dH_2O, and 5 µL (40-60 ng) of template DNA. The thermalcycler was heated to 95ºC for 2 minutes, then cooled down to 40ºC for 1 minute, then raised to 72ºC for 3 minutes. The process was repeated 30 times, and the reaction was eventually stored at 4ºC overnight.

Restriction Enzyme Digestions

These digestions were performed with 5 µL of NEB Buffer 2, 5 uL 10x BSA, and 2 uL of each Restriction Enzyme. Solutions containing plasmids pCS26, pMNOtr, pMNOpc, or insert to be digested, were used to bring the total reaction volume to 50 µL. The reaction was incubated at 37ºC for 2 hours, then heat inactivated at 65ºC for 30 minutes. 2 uL of Calf Intestine Alkaline Phosphatase (CIP) was added to digestions of plasmids, and incubated overnight at 37ºC. Digestions of pMNOtr inserts and pMNOpc insert were not dephosphorylated.

Agarose Gel Electrophoresis

Samples for electrophoresis were prepared in 12 µL volumes, containing 10 µL of plasmid or insert to be purified, and 2 uL of 6x loading dye. Ladders for the gel were prepared using 2 uL of NEB 100 bp or 1 kbp ladders, 1 µL of 6x loading dye, and 3 µL

of 1x TAE running buffer. Agarose gels were made by adding 25 mL of 1x TAE running buffer, and 0.25 or 0.75 grams of agarose to make 1% or 3% gels, respectively, to a 250 mL Erlenmeyer Flask. The mixture was boiled, then 3 µL of 4 ng/µL Ethidium Bromide was added to the gel. 15 uL of Ethidium Bromide was added to the Running Buffer in the gel box, then electrophoresis was initiated at 100 volts until the dye reached middle of gel.

DNA Band Purification

DNA fragments were purified from 1.0% and 3.0% agarose gels using Qiagen's Gel Purification Kit, with no modifications. Final DNA yields typically were 40-60 ng/µL, as determined by UV spectrophotometry in an HP 8452A spectrophotometer, using 10 µL of gel purified sample, and 990 µL of dH_2O, creating a 100 fold dilution. Samples were read at 260nm.

Ligation Reactions

50 ng of properly digested pCS26 DNA was mixed with a 5 fold molar excess of insert to be ligated (typically ~10 ng). 10 µL of 2x Quick Ligation Buffer was then added, as well as dH_2O to obtain a volume of 19 µL. Lastly, 1 µL of Quick T4 DNA Ligase was added. The tube was mixed thoroughly by brief centrifugation, and incubated at room temperature for 10 minutes before transformation. Buffer and Ligase were purchased from New England Biolabs.

Cellular Transformations

Transformations were performed using DH5α competent *E. coli* cells (Invitrogen) prepared by Jamie Towle, a member of Dr. Royer's lab. 50 µL aliquots of competent cells were thawed on ice before transformation. 5 µL of DNA ligation reaction to be transformed was added to 50 µL competent cells. The mixture was kept on ice for 40-60 minutes, then plated on bacto agar plates containing 50 µg/ml ampicillin. The plates were grown overnight at 37ºC. The amp^r colonies were picked the next day, grown in 50 mL Corning Conical tubes containing 15 mL of LB Broth, and 15 µL of 1000x ampicillin, and left in a 37ºC incubator/shaker overnight.

Assembly of pMNOpc Insert

DNA oligos were ordered from IDT with the idea of making double stranded pairs with large overhangs. Oligos For0, For 1, For 2, For 3, Rev 0, Rev 1, Rev 2, and Rev 3 were designed to piece together to assemble the insert shown in Figure-16.

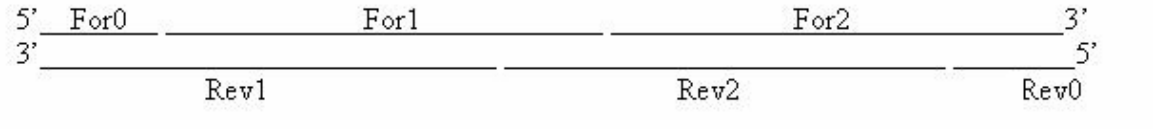

Figure 16: Assembly of a Multiple Oligo Insert. This figure shows the strategy in which multiple oligos are meant to anneal to each other to create a double stranded insert. In the scenario shown here , there are only 6 oligos, unlike the 8 oligos used to assemble pMNOpc, but the visualization and overall annealing is similar.

Pairs were annealed first (F1 to R1, F2 to R2, and F3 to R3; F0 was not annealed to R0), using 50 ng of each oligo (~100 µM final concentration of each oligo), 3 µL 10x annealing buffer (100 mM Tris-HCl, pH 7.5, 1M NaCl, 10 mM EDTA) and dH_2O. Each mixture was incubated at 95ºC for 15 minutes, and allowed to slow-cool back to room

temperature over 30-45 minutes. Each annealed oligo was purified using 2.5% agarose gel electrophoresis, then gel purified using a Qiagen gel purification kit procedures. The paired oligos, as well as short end oligos (F0 and R0) were then phosphorylated using 1 μL (10 units) of T4PolyNucleotideKinase(PNK)(New England Biolabs). All reactions were incubated at 37ºC for 1 hour, and purified using Qiagen's Nucleotide Removal Column and procedure with no modifications.

All 3 annealed oligo pairs, as well as the non annealed F0 and R0 oligos were mixed and concentrated to ~45 μL in speedvac. 5 μL of 10x Annealing Buffer was added, and the mixture was incubated at 62ºC for 30 minutes to anneal and inactivate PNK, and allowed to cool back to room temperature. DNA was purified using a 1.2% gel and Qiagen gel purification kit. The now annealed insert was then ligated and amplified using the PCR protocols previously detailed. Insert was digested with Hind III and Sac I before attempts to ligate with digested pCS26.

Transfer Vector Assembly (pMNOtr)

Transfer vector pMNOtr was assembled by cloning in pMNOtr Up and Down insert, via digestion with Hind III and NdeI/SacI, respectively. Digestion and ligation followed protocols detailed above, with each insert being digested with the proper enzyme(s) before ligation was attempted. Both inserts were ordered from IDT.

Polycistronic Vector Assembly (pMNOpc)

Polycistronic expression vector pMNOpc was assembled by digesting plasmid pCS26 with Hind III and Sac I, following protocols detailed above, and ligating with pMNOpc insert, which was assembled following the protocols above.

RESULTS

The purpose of this project was to design a polycistronic plasmid expression vector for simultaneously expressing multiple hemoglobin subunits in *E. coli* cells. The expression system was based on two key plasmids previously designed by Dr. Song Tan (Penn State University). The first part of the system consists of the transfer plasmid which is used to initially house the genes to be inserted into the polycistronic expression vector, as well as providing each of the removed cassettes with a ribosome binding site. Dr. Tan's transfer plasmid pER3aTr was modified in this project to merge its design with that of plasmid pCS26 which was previously successfully used by the Royer lab to express HbIIA and HbIIB. The new transfer plasmid was termed pMNOtr. To do this, two new inserts were needed, each containing four unique restriction enzyme sites. These inserts were termed pMNOtr Up (Figure-17) and pMNOtr Down (Figure-18), referring to their position on the plasmid with respect to the ribosome binding site. Figure 19 shows the gel purification of these up and down inserts.

Hind III BamHI EcoRI Mlu I

5'- CCC AAG CTT GGA TCC GAA TTC ACG CGT AAG CTT GGG – 3'

Fig 17: Sequence of the pMNOtr Upstream Insert. This is a visual depiction of the forward sequence of the oligonucleotide that makes up the Upstream Insert, with special respect paid to the 4 Restriction Enzyme Sites, as they are clearly noted. A fifth site for the purposes of insertion into pCS26 was unnecessary because pCS26 already contained a Hind III site that was mutated into it at an earlier point for this purpose.

Bgl II Pst I Kpn I Sac I

5’- GGA ATT CCA TAT GAT GCA TGC AGA TCT CTG CAG GGT ACC GAG CTC G – 3’

Fig 18: Sequence of the pMNOtr Downstream Insert. This is a visual depiction of the forward sequence of the oligonucleotide that makes up the Downstream Insert, highlighting the placement of the 5 Restriction Enzyme Sites. pCS26 already contained a Sac I site and Nde I site necessary for the insertion.

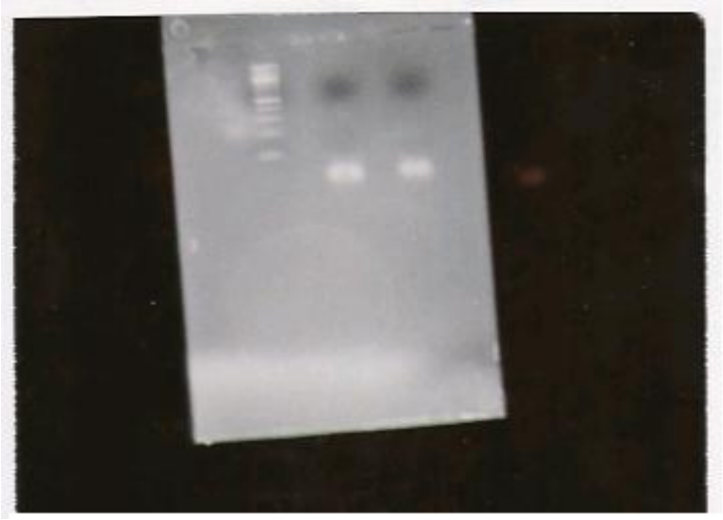

Figure 19: Gel Purification and Isolation of the Up and Down Inserts. The lanes as shown from left to right are 100bp ladder, pMNOtr Up, pMNOtr Down.

The successful ligations of the up and down inserts into pCS26 are shown in Figure-20, and resulted in the creation of the complete transfer vector pMNOtr, whose map is shown in Figure-21). This plasmid will serve as one half of the new expression system. Each individual subunit can be placed in its appropriate cassette downstream of the Ribosome Binding Site by digesting Nde I, and the appropriate downstream restriction enzyme. For example, to insert HbIIA into Cassette A, we would digest with

Nde I and Bgl II. In a separate transfer vector, we would insert a different globin gene, HbIIB into cassette B by digesting with Nde I and Pst I.

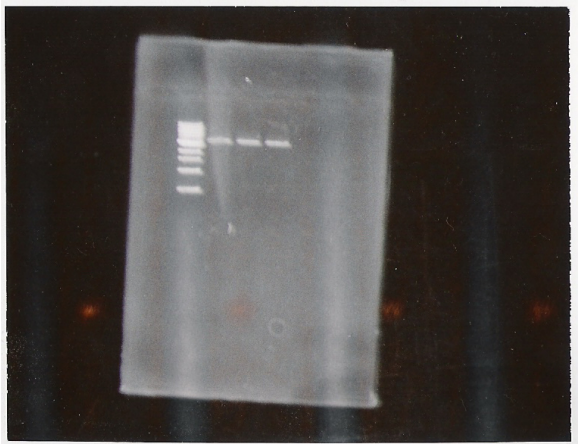

Figure 20: Agarose Gel Electrophoresis of the Completed Assemblage of Transfer Plasmid pMNOtr from pCS26. From left to right, lanes contain 1kbp ladder, and 3 different lanes of pMNOtr, all running identically and in the correct place.

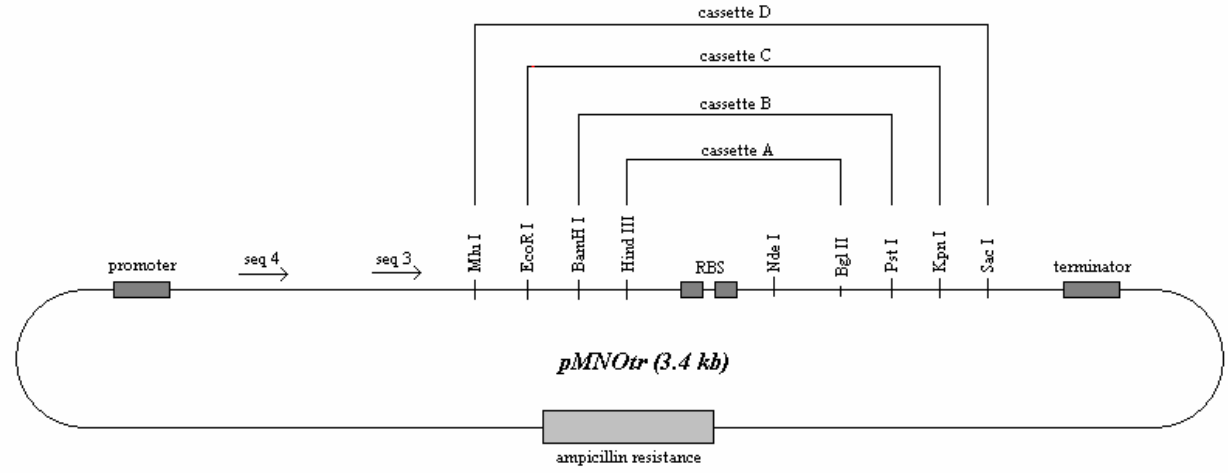

Figure 21: Complete Map of Transfer Plasmid pMNOtr. This figure represents an exaggerated model of the completed transfer vector. The various cassettes (A-D) represent the digestions to be made for removing the cassette(s) and insertion into the polycistronic vector pMNOpc, to be described below.

With the transfer vector completed, work began on creation of the polycistronic expression vector. This required a modeling of a large oligo insert with the correct restriction enzyme sites in the correct orientation with respect to the cassettes from the transfer vector (Figure-22).

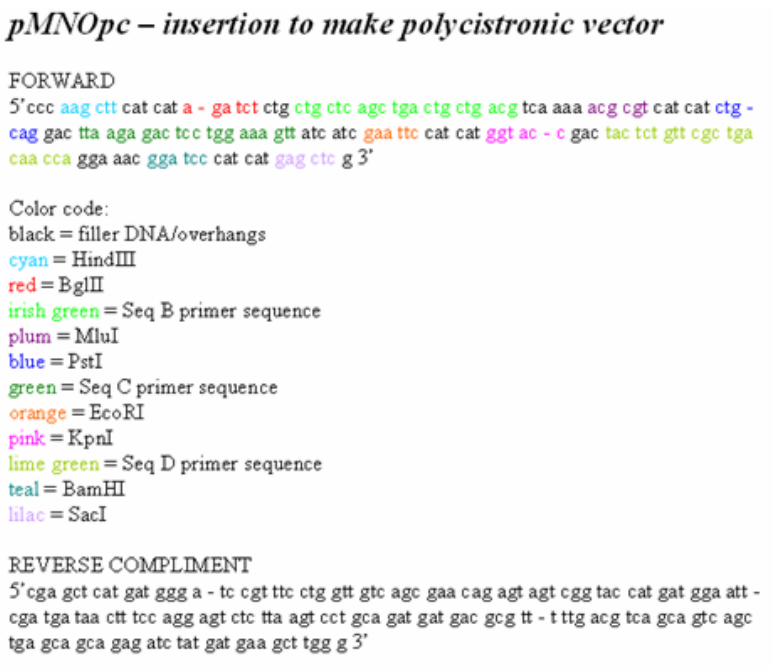

Figure 22: Sequence of the Insert Needed to Create Polycistronic Expression Vector pMNOpc. The DNA code is shown for the forward and reverse strands of pMNOpc insert. Image shows key details as to the placement of each restriction site within the overall sequence, and the location of the inserted sequencing primers.

However, ordering such a large primer would be extremely expensive and impractical. With this in mind, the total pMNOpc insert was developed as a series of 4 oligos for both the sense and antisense insert (Figure-23).

MNOpcF$_0$ = ccc aag ctt cat cat a
MNOpcF$_1$ = ga tct ctg ctg ctc agc tga ctg ctg acg tca aaa acg cgt cat cat ctg
MNOpcF$_2$ = cag gac tta aga gac tcc tgg aaa gtt atc atc gaa ttc cat cat ggt ac
MNOpcF$_3$ = c gac tac tct gtt cgc tga caa cca gga aac gga tcc cat cat gag ctc g

MNOpcR$_0$ = cga gct cat gat ggg a
MNOpcR$_3$ = tc cgt ttc ctg gtt gtc agc gaa cag agt agt cgg tac cat gat gga att
MNOpcR$_2$ = cga tga taa ctt tcc agg agt ctc tta agt cct gca gat gat gac gcg tt
MNOpcR$_1$ = t ttg acg tca gca gtc agc tga gca gca gag atc tat gat gaa gct tgg g

Seq A = gta tca cga ggc cct ttc gtc
Seq B = ctg ctc agc tga ctg ctg acg
Seq C = tta aga gac tcc tgg aaa gtt
Seq D = tac tct gtt cgc tga caa cca

Figure 23: Sequence of the 8 Oligos Used to Create the Insert for pMNOpc.

After the initial design of the oligos, each oligo had to be tested for binding potential for each other, for their intended partner, and for non-binding to the oligos they were not intended to bind. Figure-24 shows the hybridization potentials of three primer pairs, F1/R1, F2/R2, and F3/R3.

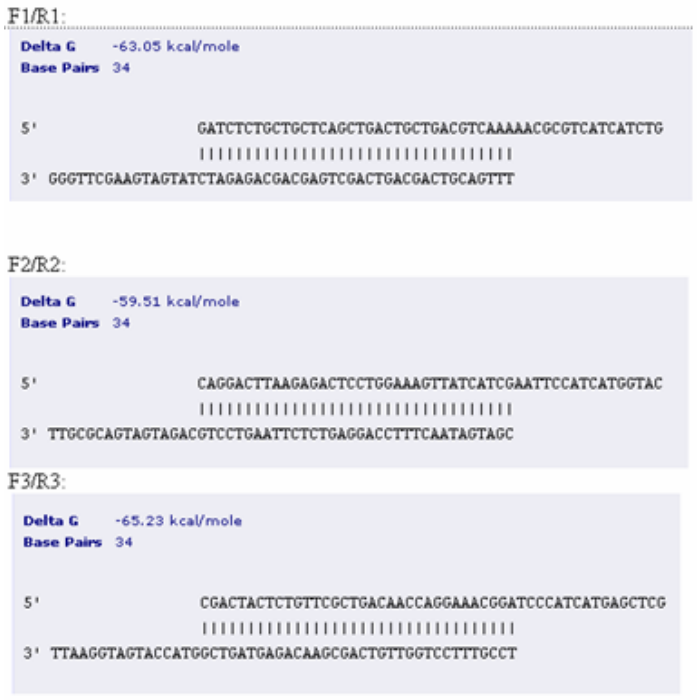

Figure 24: Binding Affinities of 6 Oligos Used to Make the Insert for pMNOpc for Each Other. This image shows the ΔG binding potential (in kcal/mol) of F1 for its intended partner R1, as well as F2 for R2, and F3 for R3.

From here, each of the inserts were annealed according to the procedures described above, resulting in the assembly of F1/R1, F2/R2, and F3/R3 complexes, as evidenced by Figure 25.

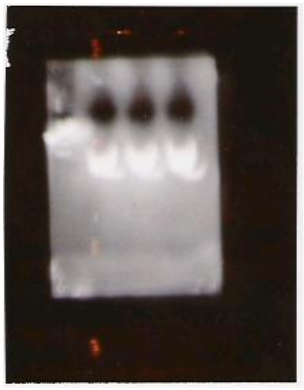

Figure 25: Electrophoresis of Assembled Oligos for the pMNOpc Insert. Shown are the migrations after the first round of oligo insert assembly. From left to right: 100bp ladder, F1/R1, F2/R2, F3/R3.

Electrophoresis of the assembled F1/R1, F2/R2, F3/R3 mixture is shown in Figure-26. The addition of oligos F0 and R0 to the assembled insert resulted in the fully assembled polycistronic insert for pMNOpc.

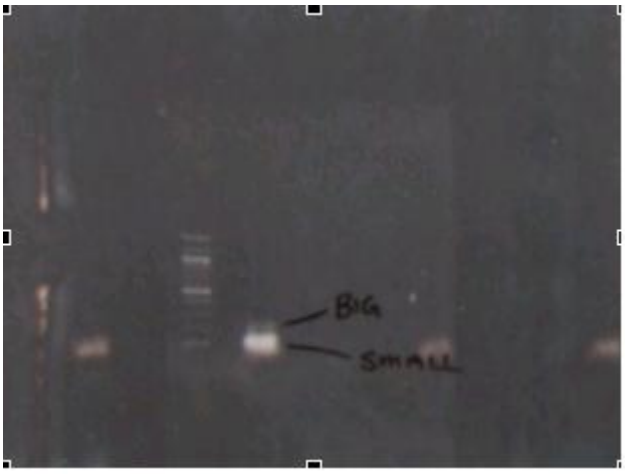

Figure 26: Electrophoresis of the Fully Assembled pMNOpc Insert. The big band (upper arrow) represents the fully assembled insert, while the smaller and brighter band (lower arrow) represents the incomplete fragments of the insert.

From here, the insert was purified and digested (Figure-27) for eventual insertion into pCS26 to assemble pMNOpc.

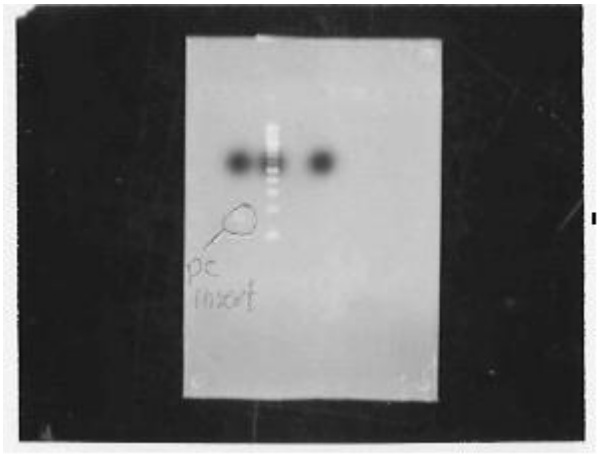

Figure 27: Digested and Fully Annealed pMNOpc Insert. Shown is the insert ready to be purified and inserted into pCS26 to create pMNOpc.

As of the time of submission of this report, the insertion of the fully annealed pc insert has not been successful, but constant attempts to complete assemblage of pMNOpc, whose map is shown in Figure-28, will continue. When the polycistronic vector is completed, globin genes will be inserted in that expression vector by digesting the transfer pMNOtr cassettes as shown in Figure-21. For example, to remove HbIIA from cassette A, we would digest with Hind III and Bgl II, picking up the desired globin gene, as well as pCS26's Ribosome Binding site, termed Cassette A. We would then digest the completed polycistronic vector with Hind III and Bgl II, inserting Cassette A from the transfer vector into the Cassette A slot on the polycistronic vector. Cassette B from the transfer vector would be inserted by digestion of the proper transfer vector with BamHI and Pst I. The procedure will be repeated until all the cassettes on the polycistronic

vector are filled, with the eventual result of the polycistronic vector being: Promoter, RBS, Gene A, RBS, Gene B, RBS, Gene C, RBS, Gene D, and the Terminator.

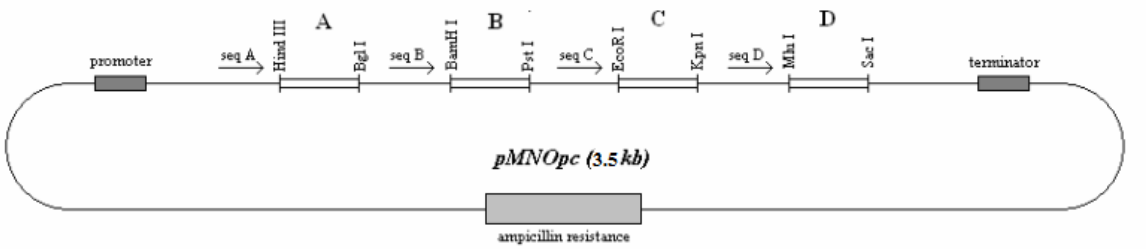

Figure 28: Diagram of Polycistronic Expression Plasmid pMNOpc. This image demonstrates what pMNOpc will look like after insertion of the pMNOpc insert into pCS26. Special attention will be paid to cassettes A-D as they precisely correlate to the assemblages demonstrated in Figure 21, pMNOtr.

DISCUSSION

The work presented here provides the framework for simultaneous expression of multiple protein subunits. With the molecular cloning and digestions a success, we can now take the next step forward in lab by using our transfer and polycistronic vectors to express various hemoglobin proteins. By creating a viable method to co-express multiple subunits of a protein, we hope to have increased both the efficiency and yield of the expressions. The presence of both subunits is necessary for complete assembly of the tetramer to take place in *E. coli*, a phenomenon not possible without co-expression.

The expression system is based on the construction of two plasmids. The transfer vector is intended to be used in the initial cloning of the globin genes, and is constructed to provide key restriction sites that precisely match various cassettes in the expression vector. The transfer vector also provides a ribosome binding site (RBS) which acts as a translational start site for each gene cassette. The expression vector consists of multiple cassette receiving sites, and provides a means to express a single mRNA, as opposed to 4 different ones, which should in theory lead to a major increase in yield, efficiency, and allow for the best possible expression of multi subunit proteins. The expressions would also not require multiple antibiotics to select for each plasmid, further increasing the chances of a successful synthesis.

The theoretically simple process of molecular cloning turned out to be anything but over the course of this project. Countless trials were required to garner the smallest of successes when it came to ligation after digestions with respect to the formation of the transfer vector. Problems were also encountered with the sequencing primer, resulting in

the resending of entire sets of samples due to the primer not reading, or the samples themselves not reading, costing valuable time and resources.

During sequencing downtime, ideas for how to improve the design became a real focus. One of the largest problems with the usage of the transfer vector is that it made our polycistronic vector unchangeable. The problem is that with each removal of a cassette, we use an expanding set of restriction sites, so by removing Cassette D, we would not just pick up MluI and Sac I sites, but would also pick up the EcoR1, BamHI, Hind III, Nde I, Bgl II, Pst I, and Kpn I sites. That means it would be impossible to edit any of the cassettes containing these sites, or in other words, cassettes A-C. Each cassette must be inserted into the polycistronic vector in the proper order of A-D descending to be done at all, otherwise the restriction digestion of the polycistronic vector would remove a previously cloned cassette. Once inserted, a gene bearing cassette could not be edited without cleaving in multiple places all of the previously inserted cassettes. This would eliminate the ability to alter the genes that could prove to be troublesome in expression, and it would be impossible to remove just one gene from the vector, resulting in having to redigest and reinsert up to 4 genes to make a change to just one.

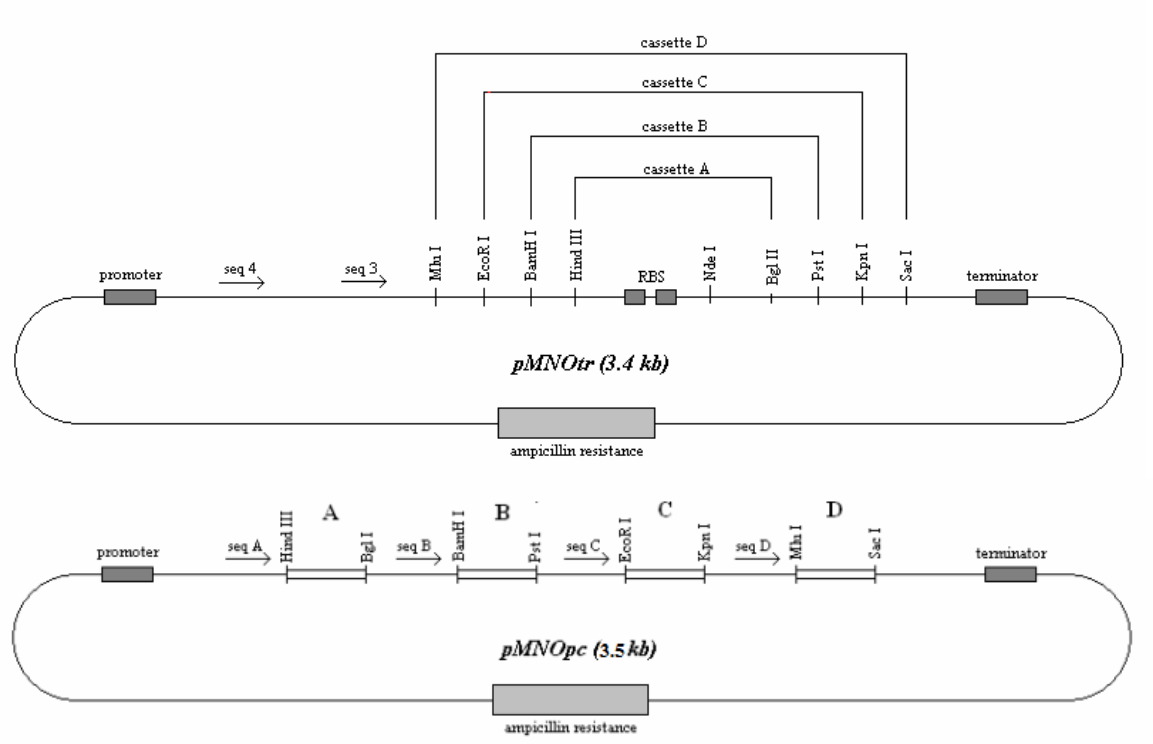

To combat this, discussion of a different idea began, in which extra restriction enzyme sites would be eliminated, allowing for editing of genes after insertion into the polycistronic vector. This would be done using the original pCS26 vector successfully tested in the Royer lab, containing the Nde I and Sac I restriction sites. The gene of interest would be inserted using an Nde I and Sac I digestion (after being appropriately designed and digested to fit into such an opening). The gene-specific primer downstream of the ribosome binding site would be designed specifically complimentary to the 3' end of the gene, and would anneal facing toward the RBS. It would then be possible to put whatever restriction enzyme site on the end of the primer that we wanted, for example, Sac I.

A primer would also be designed to lay down upstream of the RBS, facing down toward the RBS (the primers would face toward each other). From here, PCR

amplification on the gene filled vector would be performed. This would result, in theory, in a large amount of the cassette of interest, but most importantly, would remove any of the excess cut sites that were a hallmark of trouble when using the transfer vector. Our amplified insert would contain the correct restriction sites on the end, able to be digested to create the sticky/staggered ends necessary for ligation, it would have the pCS26 RBS, which is vital to having multiple Internal Ribosome Entry site, and would contain the given gene of interest. This would create a polycistronic vector without the repeated cut sites present in the cassettes added from pMNOtr, allowing for removal and non sequential (cassettes can be inserted and removed independetly of one another) editing of cassettes from pMNOpc, which would not be possible under the current system. Another boon would be using a high concentration of PCR insert, hopefully >100 ng/uL, which would greatly increase the chances of success in our ligation of the insert into the vector.

Lastly, it is our distinct hope that once the current system of transfer and polycistronic vector are completed we can run a series of hemoglobin expressions using different vectors to show the superioity of efficiency and yield as a result of our expression system. We plan on running an expression using a gene inserted into Dr. Tan's vector, pST39, a series of individual subunit expressions using an unmodified version of pCS26, and finally, an expression using MNOtr and MNOpc from pCS26. This will allow us to test the hypothesis that a polycistronic vector is superior for bacterial expression of unlike hemoglobin subunits over any other we had tried, and provide a foundation for future experiments and designs of polycistronic expression systems.

BIBLIOGRAPHY

Ackers GK, Dalessio PM, Lew GH , Daugherty MA, Holt JM (2002) Single Residue Modification of Only One Dimer Within the Hemoglobin Tetramer Reveals Autonomous Function. *PNAS* **99:** 9777-9782.

Antonini E (1967) Hemoglobin and its Reaction with Ligands. *Science* **158:** 1417-1425.

Antonini E, Ascoli F, Brunori M, Chiancone E, Verzili D, Gibson QH, Morris RJ (1984) Kinetics of Ligand Binding and Quaternary Conformational Change in the Homodimeric Hemoglobin from Scapharca inequivalvis. *Journal Biological Chemistry* **259:** 6730-6738.

Beychok S, Blout ER (1961) Optical Rotatory Dispersion of Sperm Whale Ferrimyoglobin and Horse Ferrihemoglobin. *Journal Molecular Biology* **3:** 769-777.

Bohr C, Hasselbach K, Krogh A (1904) Ueber einen in biologischer beziehung wichtigen einfluss, den die kohlensäurespannung des blutes auf dessen sauerstoffbindung übt. *Skand. Arch. Physiol.* **16:** 402-412.

Chiancone E, Vecchini P, Verzili D , Ascoli F, Antonini E (1981) Dimeric and Tetrameric Hemoglobins from the Mollusc Scapharca inequivalvis *J. Molecular Biology* **152:**577-592.

Cullis AF, Muirhead H, Perutz MF, Rossman RG, North CT (1962) Structure of Haemoglobin 3-Dimensional Fourier Synthesis at 5.5 A Resolution. *Proc. Roy. Soc. London Ser.* **263:** 161-187.

Dickerson RE, Geis I (1982) Hemoglobin. Benjamin/Cummings Publishing Co. pp. 40.

Ghisotti F, Rinaldi E (1976) Osservazioni sulla popolazione di Scapharca insediatasi in questi Ultimi anni su un tratto del litorale romagnolo. *Conchiglie, Milano* **12:** 183-191.

Gibson QH (1959) The Kinetics of Reactions Between Haemoglobin and Gases. *Progressive Biophysics and Biophysical Chemistry* **9:** 1-18.

Haurowitz F (1938) Das Gleichgewicht zwischen Hamoglobin and Sauerstoff. Hoppe Seylers Z. Physiol. Chem. **254**:266-274, as discussed in the "Eight Day of Creation" by H. F. Judson. Pg. 535-536.

Kendrew JC, HC Watson, BE Strandberg, Dickerson RE, DC Phillips, VC Shore (1961) Structure of Myoglobin: A Three-Dimensional Fourier Synthesis at 2A Resolution. *Nature* **190:** 666-670.

Knapp JE, Bonham MA, Gibson QH, Nichols JC, Royer WE (2005) Residue F4 plays a key role in modulating Oxygen affinity and cooperativity in Scapharca dimeric hemoglobin. *Biochemistry* **44:** 14149-14430.

Monod J, Wyman J, Changeux JP (1965). On the nature of allosteric transitions: a plausible model. *J. Mol. Biol.* 12: 88-118.

Perutz MF, Bolton W, Diamond P, Muirhad H, Watson HC (1964) An X-Ray Examination of Reduced Horse Haemoglobin. *Nature*. **203:** 687-690.

Royer WE, Pardanai A, Gibson QH, Peterson ES, Friedman JM (1996) Ordered Water Molecules as Key Allosteric Mediators in Cooperative Dimeric Hemoglobin. *PNAS* **93:** 14526-14531.

Royer, William (2007) Personal Communication.

Summerford C M, Pardanani A, Betts AH, Poteete AR, Colotti G, Royer WE (1995) Bacterial Expression Of *Scapharca* Dimeric Hemoglobin: A Simple Model System For Investigating Protein Cooperativity. *Protein Eng*. **8**:593-599

Tan S (2001) A modular polycistronic expression system for overexpressing protein complexes in Escherichia coli. *Protein Expression and Purification* **21:** 224-234.